$(d-2)$-Dimensional Edge States of Rotation Symmetry Protected Topological States

Zhida Song,[1,2] Zhong Fang,[1,3] and Chen Fang[1,*]
[1]*Beijing National Laboratory for Condensed Matter Physics and Institute of Physics, Chinese Academy of Sciences, Beijing 100190, China*
[2]*University of Chinese Academy of Sciences, Beijing 100049, China*
[3]*Collaborative Innovation Center of Quantum Matter, Beijing 100084, China*

(Received 14 August 2017; revised manuscript received 1 October 2017; published 11 December 2017)

We study fourfold rotation-invariant gapped topological systems with time-reversal symmetry in two and three dimensions ($d = 2, 3$). We show that in both cases nontrivial topology is manifested by the presence of the $(d-2)$-dimensional edge states, existing at a point in 2D or along a line in 3D. For fermion systems without interaction, the bulk topological invariants are given in terms of the Wannier centers of filled bands and can be readily calculated using a Fu-Kane-like formula when inversion symmetry is also present. The theory is extended to strongly interacting systems through the explicit construction of microscopic models having robust $(d-2)$-dimensional edge states.

DOI: 10.1103/PhysRevLett.119.246402

Introduction.—A symmetry protected topological state (SPT) is a gapped quantum state that cannot be continuously deformed into a product state of local orbitals without symmetry breaking [1–3]. The SPT is known to have gapless boundary states in one lower dimension [4], i.e., the $(d-1)$-dimensional edge, such as the spin-1/2 excitations at the end of a Haldane chain [5] or the Dirac surface states at the surface of a topological insulator [6,7]. The gapless states are protected by the symmetries on the $(d-1)$-dimensional edge, and when the symmetry is a spatial symmetry, they appear only on the boundary that is invariant under the symmetry operation [8–11].

Very recently, the possibility of having a gapped $(d-1)$-dimensional edge but a gapless $(d-2)$-dimensional edge has been discussed [12–15]. In Ref. [12], it was shown that, in a 2D spinless single-particle (i.e., no spin-orbit coupling) system that has anticommuting mirror planes, all four side edges can be gapped without symmetry breaking on an open square, but there are four modes localized at the four corners (0D edge) protected by mirror symmetries. Here we first extend the theory of 0D-edge states to spin-1/2 fermion systems without mirror symmetries but with fourfold rotation symmetry and time-reversal symmetry. We point out that the presence of 0D-edge states can be understood as the result of a mismatch between the locations of the centers of the Wannier states and those of atoms. Then we generalize the theory to 3D and define a new topological invariant by classifying the "spectral flow" of the Wannier centers between the $k_z = 0$ and the $k_z = \pi$ slices in the Brillouin zone. When this invariant is nontrivial, there are four helical edge modes on the otherwise gapped side surfaces of the 3D system. We further show that, when space inversion is also present, there is a Fu-Kane-like formula [16] relating this invariant to certain combinations of rotation and inversion eigenvalues of the filled bands at high-symmetry crystal momenta. Finally, we generalize the theory to strongly interacting systems, by constructing microscopic models of boson and fermion SPT states that have $(d-2)$-dimensional edge states for $d = 2, 3$ using coupled wire construction. We remark that these edge states, protected by C_4 and some local symmetry such as time reversal, are not pinned to the corners or hinges of the system and can even appear in geometries having smooth side surfaces.

Mismatch between the atom sites and the Wannier centers.—Wannier functions for the filled bands can be constructed for all 2D gapped insulators that have a zero Chern number [17]. When symmetries are involved (time reversal and/or spatial), the set of Wannier functions may or may not form a representation of the symmetry group [18]. If they do, then we call these Wannier functions "symmetric." If a set of symmetric Wannier functions cannot be found for all filled bands, we know that the system cannot be adiabatically deformed into an atomic insulator: This is considered a generalized definition of topologically nontrivial insulators [19,20], since atomic orbitals automatically form a set of symmetric wave functions. Atomic insulators are usually considered trivial. Nevertheless, we realize that even they can also be somewhat nontrivial if there is a mismatch between the Wannier centers and the atomic positions, as shown in the left panel in Fig. 1(a). A Wannier center (WC) can be understood as the middle of the Wannier function (but see Ref. [21] for a rigorous definition), and, if the Wannier functions are symmetric, their centers are also symmetric. When the mismatch happens, it means that, while the insulator can be deformed into some atomic insulator, it would *not* be made by the atoms forming the lattice. The presence of 0D-edge states of the system put on an open disk is the manifestation of the "mismatch."

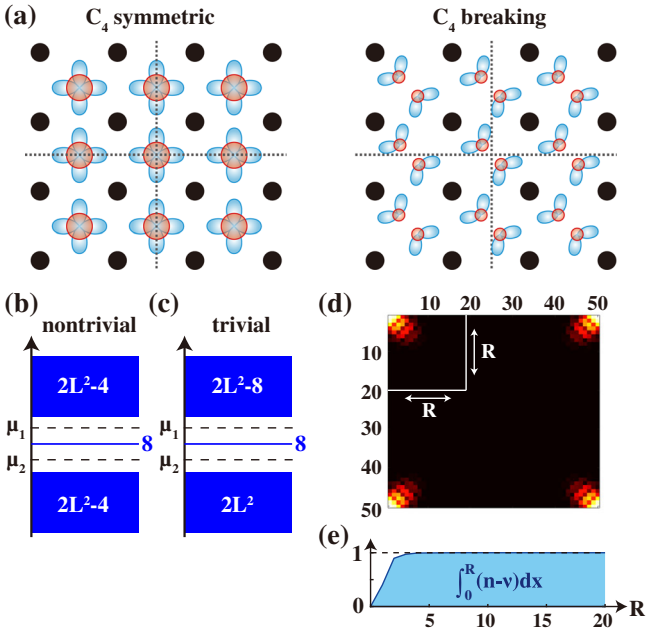

FIG. 1. Nontrivial 0D-edge modes of a 2D fermion. In (a), we sketch the mismatch between the atom sites and the WCs in the presence (left panel) and the absence (right panel) of C_4, where the atom sites are represented by the block circles and the WCs are represented by the colored orbitals. In (b) and (c), level counting for systems with nontrivial and with trivial 0D-edge state is shown, respectively. In (d), the numerical calculated density profile of the 2D model with a finite size of 50×50 is plotted, where the Fermi level is set at μ_1. The four bright regions in (d) show the additional charges located at the corners. To count the number of additional charges around a corner, we plot the integral of the density deviation from the filling ($\nu = 4$) in (e).

To be specific, let us consider a square lattice model

$$H = (1 - \cos k_x - \cos k_y)\tau_0\sigma_z s_0 + \sin k_x \tau_0\sigma_x s_x + \sin k_y \tau_0\sigma_x s_y + \Delta(\cos k_x - \cos k_y)\tau_y\sigma_y s_0, \quad (1)$$

in which all the atomic orbitals are put on the lattice sites. Here τ_i and σ_i ($i = 0, x, y, z$) are Pauli matrices representing the orbital degrees of freedom, and s_i ($i = 0, x, y, z$) representing the spin. This model can be thought of as two copies of 2D topological insulator plus a mixing term with Δ as the coefficient; and it has time-reversal symmetry $T = -is_y K$ and a rotation symmetry $C_4 = \tau_z e^{-i\pi s_z/4}$. The system put on a torus is fully gapped, because the four terms in Eq. (1) anticommute with each other and their coefficients do not vanish at the same time.

As shown in Ref. [21], whatever value Δ takes, the insulator is equivalent to an atomic one, and its WCs are located at the plaquette centers. We have explicitly constructed a set of symmetric Wannier functions and prove that, protected by the time-reversal and C_4 symmetries, the Wannier centers stay invariant under any gauge transformation that keeps the Wannier functions symmetric. This model hence realizes the mismatch between the WCs at plaquette centers and the atomic positions at sites.

Now we cut along the dotted lines in the left panel in Fig. 1(a) and turn the 2D torus into an open square. Since this cut preserves C_4 symmetries, the states centered at the plaquette center will be equally divided into four quarters, so that each quarter carries one extra electron on top of some even integer filling. Because of T, this means that a pair (Kramers's pair) of zero modes are located near each of the four corners of the square. One may observe that, in the absence of particle-hole symmetry (which is an accidental symmetry of the model), the modes can be moved away from zero and pushed into the bulk states, but we argue that, even when this happens, the corners are still nontrivial in the following sense. The total eight modes (two near each corner) come from both the conduction and the valence bands, each having $(N_{\text{band}} - \nu)L^2 - 4$ and $\nu L^2 - 4$ electrons, respectively, where $N_{\text{band}} \in$ even and $\nu \in$ even are the total number of bands and the filling number, respectively, and L the length of the square [Fig. 1(b)]. No matter where the Fermi energy is, a gapped ground state must have 4 mod 8 electrons on an even-by-even lattice, so that each corner has exactly one (or minus one) extra electron on top of the filling of the bulk. This is in sharp contrast with the systems having trivial corner states, whose energy levels are plotted in Fig. 1(c). In that case, the in-gap states can be pushed into the conduction bulk, and there is no extra charge at each corner. In Figs. 1(d) and 1(e), we plot the charge density at $\mu = \mu_1$ in real space and plot the extra electric charge within a small area near the corner as a function of radius in the Slater-product many-body ground state.

To see how the odd parity of the corner charge is protected by C_4, we contrast the above scenario with the one having a nematic perturbation breaking C_4 down to C_2, so that the Wannier centers are shifted to the positions shown in the right panel in Fig. 1(a). When the system is cut along the dotted lines, the quarter has inside it an integer number of Kramers' pairs, and the degeneracy at each corner is absent.

1D helical state and $\mathbb{Z}_2$ Wannier center flow.—A natural generalization of the 0D state in 2D is the 1D-edge state in 3D, where both the 3D bulk and 2D side surfaces are insulating, as shown in Fig. 2(c). Our construction of this state is also based on the WC picture. Assuming the 3D system has T and C_4 symmetries, we can take a C_4-invariant tetragonal cell and transform the Hamiltonian along the z direction to momentum space. Each slice with fixed k_z can be thought of as a 2D system, wherein the $k_z = 0, \pi$ slices are time reversal and C_4 invariant, while the others are only C_4 invariant. Consider an insulator that has four filled bands, or four WCs for each k_z slice. Because of C_4, the four WCs are related to each other by fourfold rotations; and due to T, at $k_z = 0$ or $k_z = \pi$, two WCs that form a Kramers's pair must coincide. Therefore, at $k_z = 0$

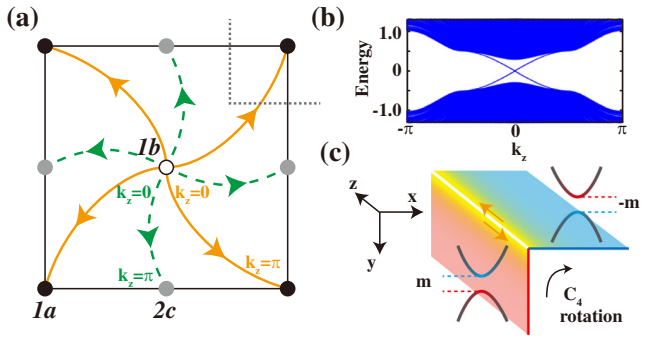

FIG. 2. Nontrivial 1D helical modes of a 3D insulator. In (a), we plot the two generators of nontrivial $\mathbb{Z}_2$ flows from the $k_z = 0$ slice to the $k_z = \pi$ slice, where the lattice site ($1a$), the plaquette center ($1b$), and the edge midpoint ($2c$) are represented by a black planchet, hollow circle, and gray planchet, respectively. In (b), the numerically calculated helical modes of our 3D model on a tetragonal cylinder geometry are plotted. The length along the x and y directions is 50. In (c), we sketch the domain wall between surfaces of opposite masses, enforced by the C_4 rotation symmetry.

and $k_z = \pi$, there are only three possible configurations for the four WC: all four at $1a$, all four at $1b$, and two at each $2c$ Wyckoff position. Wyckoff positions are points in a lattice that are invariant under a subgroup of the lattice space group. For a square lattice in a Wigner-Seitz unit cell, $1a$ and $1b$ are the center and the corner invariant under C_4, $2c$ are the middles of the edges invariant under C_2, and $4d$ are generic points invariant under identity (the trivial subgroup). If the configurations at $k_z = 0$ and at $k_z = \pi$ are different, the evolution of the WC between the two slices forms a "$\mathbb{Z}_2$ flow," a robust topological structure revealing that the 3D insulator is not an atomic one. Out of several different combinations of the configurations at $k_z = 0$ and $k_z = \pi$, there are two topologically distinct $\mathbb{Z}_2$ flows, where the four WCs flow from $1b$ to $1a$ and from $1b$ to $2c$ [solid yellow and dashed green lines in Fig. 2(a)], respectively. The latter $\mathbb{Z}_2$ flow can be shown equivalent to a weak topological index (Ref. [21]), and we from now on focus on the first $\mathbb{Z}_2$ flow from $1b$ to $1a$. Whether this flow is present or not gives us a new $\mathbb{Z}_2$ invariant, and its edge manifestation is the existence of 1D helical edge modes on the side surface of a bulk sample. (For a more rigorous definition and classification of the WC flow for an arbitrary number of filled bands, see Ref. [21].)

To see this bulk-edge correspondence, we cut the bulk along both the x and y directions, keeping the periodic boundary condition along z. From a top-down perspective, a corner of the sample takes the shape of the dotted lines shown in Fig. 2(a). One can see that, at the corner, the boundary cuts through exactly one (or three) line(s) in the WC flow, corresponding to one helical mode along the hinge between the two open surfaces. To make the picture more concrete, we consider the following 3D model, which is a simple extension of the 2D model in Eq. (1):

$$H = \left(2 - \sum_i \cos k_i\right)\tau_0\sigma_z s_0 + \sum_i \sin k_i \tau_0 \sigma_x s_i + \Delta(\cos k_x - \cos k_y)\tau_y\sigma_y s_0. \quad (2)$$

The $k_z = 0$ slice is equivalent with the 2D model in Eq. (1), thus having four charges locating at the plaquette center. The $k_z = \pi$ slice is, however, a 2D atomic insulator with four charges locating at the lattice site. The mismatch between the WCs at $k_z = 0$ and $k_z = \pi$ slices means that the $\mathbb{Z}_2$ flow exists. To confirm the $\mathbb{Z}_2$ flow, we also choose a smooth gauge for all the k_z slices from $k_z = 0$ to $k_z = \pi$ and plot the WC flow explicitly, which indeed gives the $\mathbb{Z}_2$ flow, shown in Ref. [21]. The 1D helical state is also confirmed by a numerical calculation of the band structure of a finite tetragonal cylinder, as plotted in Fig. 2(b). For this particular model, the helical edge states can be viewed from another perspective. The edge between the two open surfaces can be considered as the domain wall between them. On each surface there is a mass gap, and the rotation symmetry in this model enforces the two masses to be opposite, so that at the domain wall there is a helical mode [11] [see Fig. 2(c) for a schematic, and see Ref. [21] for more details].

Symmetry indicators for the $\mathbb{Z}_2$ invariant.—To see if a given insulator has 1D helical edge modes on the side surface, one needs to calculate the evolution of the WCs as a function of k_z, which in turn requires finding symmetric, smooth, and periodic Bloch wave functions for all bands at each k_z slice as is done for our model Hamiltonian. This is practically impossible in real materials. Now we show that, in the presence of additional inversion symmetry, this $\mathbb{Z}_2$ invariant can be determined by the rotation and inversion eigenvalues at all high-symmetry momenta, simplifying the diagnosis. We call this method a "Fu-Kane-like formula," likening it to the Fu-Kane formula for time-reversal topological insulators [16], where inversion is not required to protect the nontrivial topology but when present greatly simplifies the calculation.

This formula is derived based on the new theory of symmetry indicators [19,20]: Given any insulator, a full set of eigenvalues of the space group symmetry operators for filled bands at all high-symmetry points generates a series of indicators. They tell us if this set is consistent with any atomic insulator, and, if yes, the theory further gives where the atomic orbitals are located. Our goal is to find such an indicator that is equivalent to the $\mathbb{Z}_2$ invariant for the WC flow. Following the WC flow picture, we require (i) at $k_z = 0$ and $k_z = \pi$, the eigenvalues of C_4, $C_2 = C_4^2$ and P are consistent with atomic insulators; (ii) there is no surface state on the side surfaces; and (iii) comparing the two slices at $k_z = 0$ and $k_z = \pi$, the numbers of atomic orbitals at $1a$ and at $1b$ change by ± 4 and ∓ 4, respectively. For a concrete example, let us consider space group $P4/m$, whose indicators form a group $\mathbb{Z}_2 \times \mathbb{Z}_4 \times \mathbb{Z}_8$ [19], so that

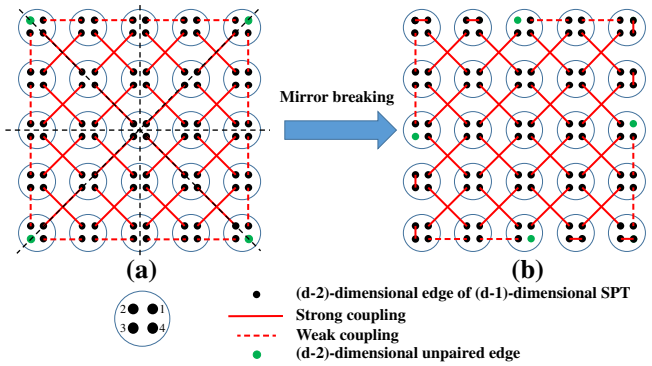

FIG. 3. Coupled wire construction for a 3D SPT with robust 1D-edge modes. Each filled circle is a wire from the top down, and each open circle including four elementary wires is a "physical" wire that can be realized in 1D lattice models. The breaking of mirror symmetry in (a) causes the edge modes to move to the positions in (b).

the insulator according to its C_4 and P eigenvalues can be denoted by (mnl) $(m = 0, 1, n = 0, 1, 2, 3, l = 0, 1, \ldots, 7)$, and an insulator with a nonzero indicator cannot be adiabatically deformed into an atomic insulator. Using the three criteria above, we find that the $\mathbb{Z}_2$ flow is nontrivial only if $(mnl) = (004)$. We have found the explicit formulas to calculate these indicators directly from the symmetry eigenvalues, which can be applied to all space groups having both C_4 and P. (See Ref. [21] for the results, and find a MATLAB script therein for an automated diagnosis for materials in these space groups.)

Extension to strongly interacting SPT.—In the above we have established the theory of $(d-2)$-dimensional edge modes for free fermions through the WC picture. Since WC is a single-particle object, the same picture does not apply for strongly interacting bosons or fermions. Here we rebuild a 3D free fermion model with robust 1D helical edge modes using coupled wire construction [24–28], a method that can be easily extended to strongly interacting SPT. These SPT can either be bosonic [29] or fermionic and are, in general, protected by spatial symmetry [30] plus some internal symmetry [31].

Consider an arrangement of 1D wires shown in the top down view in Fig. 3(a), each of which represents a helical mode. Because of the fermion doubling theorem, each wire alone cannot be physically realized in 1D, but an even number of these wires can be realized as a 1D wire fine-tuned to a critical point. In our model, four wires make a physical, critical 1D wire. For concreteness, we assume that under C_4 rotation the four wires inside cyclically permute. Then we couple the wires in the following way: The four wires, in the top down view, which share a plaquette are coupled diagonally, i.e., 1 coupled to 3 and 2 to 4. For a 3D torus, these couplings (solid red lines) make the coupled wire system an insulator. For a cylinder geometry open in the x and y directions, however, there are "dangling helical wires" on the side surfaces, which can again be gapped by turning on a dimerizing coupling (dotted lines). But one soon discovers that, as long as C_4 is preserved, there are always four unpaired wires on the side surface (represented by green dots), which are in fact the same 1D helical edge mode protected by C_4 and T studied above.

This construction can be easily extended to strongly interacting SPT. One simply replaces each helical wire with a $(d-2)$-dimensional edge of a $(d-1)$-dimensional SPT protected by some local symmetry. For example, each "wire" can be a 0D spin $1/2$, which is the edge of a 1D Haldane chain protected by SO(3) symmetry. In that case, the resultant construction in Fig. 3(a) is nothing but an Affleck-Kennedy-Lieb-Tasaki (AKLT)-like state [32,33] formed by $S = 2$ spins, but, unlike previously considered AKLT states in 2D, it has a gapped 1D edge but four 0D gapless spin-$1/2$ excitations localized at the four corners in an open square. We can also replace each wire by the edge of a Levin-Gu state [34], protected by a $\mathbb{Z}_2$ local symmetry, and then the construction in Fig. 3(a) is a 3D bosonic SPT with 1D gapless modes at four corners. Notice that, in these boson examples, time-reversal symmetry is not necessary. Similar construction can be used to obtain SPT states protected by both the local symmetries [being T, SO(3), or Z_2] and C_4-rotation symmetry.

Discussion.—It is important to note that, while in examples studied so far the $(d-2)$-dimensional edge modes sit at the corners or hinges in the disk or cylinder geometry, it is not always the case. In the model shown in Fig. 3(a), the edge modes are pinned to the corners by the mirror symmetries (dotted lines), and breaking these mirror planes in the bulk or on the surface causes the edge modes to move away. In the example shown in Fig. 3(b), we break the mirror symmetry of the construction on the surface, so that the dangling wires move from the corners to some generic points on the side. As long as C_4 is present, the $(d-2)$-dimensional edge modes are stable yet not pinned to corners or hinges in the absence of mirror symmetries. In fact, they still appear even if the whole side surface is smooth without hinges at all. We also emphasize that, while these edge modes are protected by C_4-rotation symmetry, breaking the symmetry perturbatively in the bulk or on the boundary does not, in general, gap out the modes, because time reversal alone is sufficient to protect 1D helical edge modes. The only way of gapping the modes is to annihilate them in pairs, and this means large C_4 breaking either in the bulk or on the boundary. Similar discussions may be extended to systems with twofold, threefold, and sixfold rotations.

Experimentally, the four helical edge modes of a 3D electronic insulator contribute a quantized conductance of $4e^2/h$ that may be measured in electric transport [7]. Also, the $(d-2)$-dimensional edge modes may be detected by local probes such as scanning tunneling microscopy, either on a bulk sample or at the step edge of a thin film.

C. F. thanks Xi Dai, Meng Cheng, Yang Qi, and B. Andrei Bernevig for helpful discussion. The work was

supported by the National Key Research and Development Program of China under Grant No. 2016YFA0302400 and by National Science Foundation of China under Grant No. 11674370.

Note added.—We are aware of works on related topics that have appeared on arXiv after our posting [35–37]; their results have a finite overlap with ours and seem consistent.

*cfang@iphy.ac.cn

[1] Z.-C. Gu and X.-G. Wen, Phys. Rev. B **80**, 155131 (2009).
[2] X. Chen, Z.-C. Gu, Z.-X. Liu, and X.-G. Wen, Science **338**, 1604 (2012).
[3] Y.-M. Lu and A. Vishwanath, Phys. Rev. B **86**, 125119 (2012).
[4] X. Chen, Z.-X. Liu, and X.-G. Wen, Phys. Rev. B **84**, 235141 (2011).
[5] F. D. M. Haldane, Phys. Rev. Lett. **50**, 1153 (1983).
[6] M. Z. Hasan and C. L. Kane, Rev. Mod. Phys. **82**, 3045 (2010).
[7] X.-L. Qi and S.-C. Zhang, Rev. Mod. Phys. **83**, 1057 (2011).
[8] L. Fu, Phys. Rev. Lett. **106**, 106802 (2011).
[9] A. M. Turner, Y. Zhang, and A. Vishwanath, Phys. Rev. B **82**, 241102 (2010).
[10] T. L. Hughes, E. Prodan, and B. A. Bernevig, Phys. Rev. B **83**, 245132 (2011).
[11] T. H. Hsieh, H. Lin, J. Liu, W. Duan, A. Bansil, and L. Fu, Nat. Commun. **3**, 982 (2012).
[12] W. A. Benalcazar, B. A. Bernevig, and T. L. Hughes, Science **357**, 61 (2017).
[13] F. Schindler, A. Cook, M. G. Vergniory, and T. Neupert, in Proceedings of the APS March Meeting (unpublished).
[14] R.-J. Slager, L. Rademaker, J. Zaanen, and L. Balents, Phys. Rev. B **92**, 085126 (2015).
[15] Y. Peng, Y. Bao, and F. von Oppen, Phys. Rev. B **95**, 235143 (2017).
[16] L. Fu, C. L. Kane, and E. J. Mele, Phys. Rev. Lett. **98**, 106803 (2007).
[17] N. Marzari and D. Vanderbilt, Phys. Rev. B **56**, 12847 (1997).
[18] A. A. Soluyanov and D. Vanderbilt, Phys. Rev. B **83**, 035108 (2011).
[19] H. C. Po, A. Vishwanath, and H. Watanabe, Nat. Commun. **8**, 50 (2017).
[20] B. Bradlyn, L. Elcoro, J. Cano, M. G. Vergniory, Z. Wang, C. Felser, M. I. Aroyo, and B. A. Bernevig, Nature (London) **547**, 298 (2017).
[21] See Supplemental Material at http://link.aps.org/supplemental/10.1103/PhysRevLett.119.246402 for derivation of the topological invariants, the detailed analysis of our toy model, and derivation of the Fu-Kane-like formula, which includes Refs. [22,23].
[22] S. L. Altmann and P. Herzig, *Point-Group Theory Tables* (Clarendon, Oxford, 1994).
[23] C. Fang, M. J. Gilbert, and B. A. Bernevig, Phys. Rev. B **86**, 115112 (2012).
[24] J. C. Y. Teo and C. L. Kane, Phys. Rev. B **89**, 085101 (2014).
[25] Y. Oreg, E. Sela, and A. Stern, Phys. Rev. B **89**, 115402 (2014).
[26] T. Neupert, C. Chamon, C. Mudry, and R. Thomale, Phys. Rev. B **90**, 205101 (2014).
[27] J. Klinovaja and Y. Tserkovnyak, Phys. Rev. B **90**, 115426 (2014).
[28] J. Klinovaja, Y. Tserkovnyak, and D. Loss, Phys. Rev. B **91**, 085426 (2015).
[29] R. Thorngren and D. V. Else, arXiv:1612.00846.
[30] S.-J. Huang, H. Song, Y.-P. Huang, and M. Hermele, arXiv:1705.09243 [Phys. Rev. B (to be published)].
[31] C. Wang and M. Cheng (to be published).
[32] I. Affleck, T. Kennedy, E. H. Lieb, and H. Tasaki, Phys. Rev. Lett. **59**, 799 (1987).
[33] I. Affleck, T. Kennedy, E. H. Lieb, and H. Tasaki, Commun. Math. Phys. **115**, 477 (1988).
[34] M. Levin and Z.-C. Gu, Phys. Rev. B **86**, 115109 (2012).
[35] W. A. Benalcazar, B. A. Bernevig, and T. L. Hughes, Phys. Rev. B **96**, 245115 (2017).
[36] F. Schindler, A. M. Cook, M. G. Vergniory, Z. Wang, S. S. P. Parkin, B. A. Bernevig, and T. Neupert, arXiv:1708.03636.
[37] J. Langbehn, Y. Peng, L. Trifunovic, F. von Oppen, and P. W. Brouwer, preceding Letter, Phys. Rev. Lett. **119**, 246401 (2017).